Structure–activity studies of lGnRH-III through rational amino acid substitution and NMR conformational studies

ARTICLE *in* BIOPOLYMERS · DECEMBER 2012

Impact Factor: 2.39 · DOI: 10.1002/bip.22123 · Source: PubMed

9 AUTHORS, INCLUDING:

Aikaterini Zompra
University of Patras
18 PUBLICATIONS **85** CITATIONS
SEE PROFILE

George N. Pairas
University of Patras
62 PUBLICATIONS **205** CITATIONS
SEE PROFILE

Fotini Lamari
University of Patras
89 PUBLICATIONS **1,500** CITATIONS
SEE PROFILE

Panagiotis Katsoris
University of Patras
48 PUBLICATIONS **785** CITATIONS
SEE PROFILE

Structure–Activity Studies of lGnRH-III Through Rational Amino Acid Substitution and NMR Conformational Studies

Eleni V. Pappa,[1] Aikaterini A. Zompra,[1] Zoi Diamantopoulou,[2] Zinovia Spyranti,[1] George Pairas,[1] Fotini N. Lamari,[1] Panagiotis Katsoris,[2] George A. Spyroulias,[1] Paul Cordopatis[1]

[1]*Department of Pharmacy, University of Patras, Patras 26504, Greece*

[2]*Department of Biology, University of Patras, Patras 26504, Greece*

Received 3 April 2012; revised 31 May 2012; accepted 2 July 2012
Published online 17 July 2012 in Wiley Online Library (wileyonlinelibrary.com). DOI 10.1002/bip.22123

ABSTRACT:

Lamprey gonadotropin-releasing hormone type III (lGnRH-III) is an isoform of GnRH isolated from the sea lamprey (Petromyzon marinus) with negligible endocrine activity in mammalian systems. Data concerning the superior direct anticancer activity of lGnRH-III have been published, raising questions on the structure–activity relationship. We synthesized 21 lGnRH-III analogs with rational amino acid substitutions and studied their effect on PC3 and LNCaP prostate cancer cell proliferation. Our results question the importance of the acidic charge of Asp[6] for the antiproliferative activity and indicate the significance of the stereochemistry of Trp in positions 3 and 7. Furthermore, conjugation of an acetyl-group to the side chain of Lys[8] or side chain cyclization of amino acids 1-8 increased the antiproliferative activity of lGnRH-III demonstrating that the proposed salt bridge between Asp[6] and Lys[8] is not crucial. Conformational studies of lGnRH-III were performed through NMR spectroscopy, and the solution structure of GnRH-I was solved. In solution, lGnRH-III adopts an extended backbone conformation in contrast to the well-defined β-turn conformation of GnRH-I.

Keywords: Lamprey GnRH-III; lGnRH-III analogs; solution structure GnRH-I; solution structure lGnRH-III; antiproliferative activity

This article was originally published online as an accepted preprint. The "Published Online" date corresponds to the preprint version. You can request a copy of the preprint by emailing the Biopolymers editorial office at biopolymers@wiley.com

INTRODUCTION

The decapeptide gonadotropin-releasing hormone-I (GnRH-I; pGlu-His-Trp-Ser-Tyr-Gly-Leu-Arg-Pro-Gly-NH_2) has a pivotal role in orchestrating and maintaining normal reproductive events by regulating the secretion of pituitary gonadotropin hormones.[1] In addition, GnRH-I and many of its analogs exhibit an antiproliferative effect on various cancer cells, which can be exerted by indirect or direct ways.[2–4] Chronic administration of GnRH analogs desensitizes the pituitary gonadotroph cells, results in arrest of gonadotropin secretion, and thereby suppresses ovarian and testicular function (chemical castration). Thus, chemical castration is a therapeutic approach of hormone-dependent tumors such as prostate and breast cancer. Thousands of synthetic peptide analogs of GnRH have been synthesized since its discovery, and several of them (agonists or antagonists) have been used in breast and/or prostate cancer therapy.[4] In addition, GnRH analogs also exert anticancer activity by directly affecting the hormone-dependent and -independent cancer cells, an effect which

Additional Supporting Information may be found in the online version of this article.

Correspondence to: Paul Cordopatis, Laboratory of Pharmacognosy and Chemistry of Natural Products, Department of Pharmacy, University of Patras, GR-265 04 Patras, Greece; e-mail: pacord@upatras.gr or Eleni V. Pappa, Laboratory of Pharmacognosy and Chemistry of Natural Products, Department of Pharmacy, University of Patras, GR-265 04 Patras, Greece; e-mail: el2pappa@yahoo.gr

Table I Yield of Synthesis and Physicochemical Properties of lGnRH-III Analogs

	Peptide Code	Sequence	Yield[a] (%)	HPLC[b] t_R (min)	MH^+obsd/(calcd)[c]
lGnRH-III		pGlu[1]-His[2]-Trp[3]-Ser[4]-His[5]-Asp[6]-Trp[7]-Lys[8]-Pro[9]-Gly[10]-NH_2	76.1	7.09	1260.33/1259.33
Group A	I	[Asn[6]]-lGnRH-III	69.8	7.12	1258.92/1258.35
	II	[Asp[6](OMe)]-lGnRH-III	54.8	7.58	1274.02/1273.36
	III	[Glu[6]]-lGnRH-III	71.1	7.23	1273.66/1273.36
	IV	[Gln[6]]-lGnRH-III	73.1	7.18	1272.10/1272.37
Group B	V	[DTrp[3]]-lGnRH-III	70.7	7.27	1259.70/1259.33
	VI	[DTrp[7]]-lGnRH-III	58.6	7.32	1260.23/1259.33
	VII	[DTrp[3], DTrp[7]]-lGnRH-III	67.9	7.20	1259.83/1259.33
	VIII	[DTrp[3], DTrp[7]]-lGnRH-III-NHEt	78.3	7.19	1287.92/1287.38
	IX	[Tic[3], Tic[7]]-lGnRH-III	73.2	7.14	1205.55/1205.28
	X	[DTic[3], DTic[7]]-lGnRH-III	77.8	7.23	1205.58/1205.28
	XI	[DTrp[3], DTic[7]]-lGnRH-III	74.4	6.93	1231.97/1232.31
	XII	[DTic[3], DTrp[7]]-lGnRH-III	78.5	6.83	1231.94/1232.31
Group C	XIII	[NMeGlu[1]]-lGnRH-III	81.3	7.73	1292.11/1291.37
	XIV	[cyclo(Glu[1], Lys[8])]-lGnRH-III	45.2	7.86	1276.17/1275.33
	XV	[cyclo(Ac-Glu[1], Lys[8])]-lGnRH-III	53.1	9.61	1318.14/1317.37
	XVI	[ε-*N*-Ac-Lys[8]]-lGnRH-III	80.8	7.96	1302.23/1301.37
	XVII	[Glu[1], ε-*N*-Ac-Lys[8]]-lGnRH-III	67.1	7.21	1320.19/1319.38
	XVIII	[Ac-Glu[1], ε-*N*-Ac-Lys[8]]-lGnRH-III	80.4	8.11	1362.33/1361.42
	XIX	[Lys[5], His[8]]-lGnRH-III	81.0	7.31	1259.71/1259.33
	XX	[cyclo(Glu[1], Lys[5]), His[8]]-lGnRH-III	39.1	7.43	1276.08/1275.33
	XXI	[cyclo(Ac-Glu[1], Lys[5]), His[8]]-lGnRH-III	43.7	8.60	1318.21/1317.37

[a] Yields were calculated on the basis of the amino acid content of the resin. All peptides were at least 98% pure.
[b] For elution conditions, see Materials and Methods section.
[c] Data obtained by ESI-MS, observed (obsd) and calculated (calcd) m/z values of MH^+.

could be mediated through the GnRH receptors (GnRHRs) highly expressed in those cells.

The discovery of lGnRH-III (pGlu-His-Trp-Ser-His-Asp-Trp-Lys-Pro-Gly-NH_2), a native GnRH analog isolated from sea lamprey (*Petromyzon marinus*)[5] that stimulates the release of estradiol and progesterone in the adult female sea lamprey,[6,7] has stimulated further research on their potential medicinal uses. Functional activity of lGnRH-III has been found in the hypothalamus of several (mammalian) species, including rats, cows, and sheep, and it was originally suggested that lGnRH-III might act as a mammalian Follicle-Stimulating Hormone (FSH) releasing factor.[8–11] However, the data concerning the effect of lGnRH-III on the selective secretion of FSH are inconsistent.[12–14] While questions concerning the endocrine activity of lGnRH-III are yet not answered, studies concerning the direct anticancer activity of lGnRH-III have been published in the last decade.[15–18] lGnRH-III differs in the sequence 5-8 from the mammalian GnRH (GnRH-I)[5] and is a weak agonist of the mammalian GnRHR. The ability of lGnRH-III to inhibit proliferation of cancer cells, combined with the weak GnRH-I agonistic activity, makes it an excellent starting compound for the development of peptide analogs with high and selective anticancer activity. Currently, new GnRH analogs have been synthesized to enhance the anticancer potency of native lGnRH-III.[5,13,16,17] Those studies have shown that modifications in positions 5-8 decrease the anticancer activity of lGnRH-III. Systematic replacement of residues 5-8 of lGnRH-III by Ala[19] showed that mutation of Asp[6] or Trp[7] resulted in the loss of antiproliferative effect probably due to an ionic interaction between these residues, which might stabilize the biologically active conformation of lGnRH-III. In addition, the importance of indole rings of Trp[3,7] was also proposed.[16] However, further information on the structure–activity relationships of lGnRH-III is still lacking.

To further investigate the structure–activity relationship of lGnRH-III, we synthesized 21 new lGnRH-III analogs and studied their direct antiproliferative effect on prostate cancer cells. The analogs were arranged into three groups: (A) analogs with single amino acid changes in position 6, (B) analogs with modifications in positions 3 and/or 7, (C) analogs with amino acid changes in positions 1, 5, 8 and cyclic analogs (Table I). In particular, we studied the importance of the Asp in position 6 by incorporation of several amino acids [Asn, Asp(OMe), Glu, Gln]. DTrp and L/D-1,2,3,4-tetrahydroisoquinoline-3-carboxylic acid (Tic) were inserted in positions 3 and/or 7 to further investigate the role of the

indole ring of Trp and its stereochemistry. In the last group, the importance of the amino acids in positions 1 and 8 are mainly studied. The utility of backbone cyclization has been well established in peptides, and it has been demonstrated to increase biological activity and selectivity[20,21] since they are usually more stable in metabolism than the parent linear molecules.[22] Therefore, cyclopeptides are of great importance and interest both in pharmaceutical and chemical respect. According to these considerations, we also synthesized 1-8 and 1-5 side chain cyclic peptides and studied their antiproliferative activity on prostate cancer cells.

Moreover, until today, some sporadic attempts have been done to study the solution conformation of lGnRH-III, but there is still no NMR 3D model available. According to the results of a previous molecular dynamics simulation study by Lovas and coworkers,[23] lGnRH-III has an extended helical conformation from residues 2 through 7, which is stabilized by intramolecular hydrogen bonds and slightly polar interactions. However, that conformational model has not been confirmed by other studies.[17] The determination of the conformational characteristics of lGnRH-III is a crucial step for in depth study of structure–activity relationship. In that direction, we studied the solution structure of lGnRH-III through NMR spectroscopy, and a conformational model of this decapeptide is presented. Moreover, the solution structure of GnRH-I (PDB 1YY1) was studied under the same experimental conditions to elucidate the conformational differences between GnRH-I and lGnRH-III.

MATERIALS AND METHODS

Peptide Synthesis

The linear and the cyclic peptides (Table I) were rationally designed and synthesized manually. 9-Fluorenylmethoxycarbonyl (Fmoc)-protected amino acids and peptide reagents were obtained from CBL (Patras, Greece), Bachem (Bubendorf, Switzerland), and Novabiochem (Läufelfingen, Switzerland). All solvents and reagents used for solid-phase synthesis were of analytical quality. Purification of crude peptides was achieved by semipreparative high-performance liquid chromatography (HPLC) (Mod.10 ÄKTA, Amersham Biosciences, Piscataway, NJ) coupled to a UV/Vis detector from Amersham Pharmacia Biotech on a Supelcosil C18 (5μm particle size, 8 mm × 250 mm, Sigma-Aldrich, St Louis, MO). Analytical HPLC (Waters, Malva, Milford, CT) equipped with a Waters C18 column (symmetry, 3.5 μm, 4.6 mm × 75 mm) produced single peaks with at least 98% of the total peak integrals (integrated with Empower software). Electrospray ionization-mass spectrometry (ESI-MS, Micromass-Platform LC instrument, Waters Micromass Technologies, Milford, MA) was in agreement with the expected mass. The physicochemical properties of the new analogs are summarized in Table I.

Linear Peptides. Sieber amide resin (0.45 mmol/g capacity) was used as a solid support for the linear peptides. All peptides were synthesized manually following a Fmoc strategy. First, the Fmoc protecting group on the resin was removed by treatment with 20% piperidine/*N*,*N*-dimethylformamide (DMF) and then, the coupling reaction was performed by using threefold molar excesses of activated Fmoc-amino acids throughout the synthesis. The amino acids were activated essentially either in situ using diisopropylcarbodiimide/1-hydroxy-benzotriazol (HOBt) in DMF for 2.5 h or with *O*-benzotriazol-1-yl-1,1,3,3-tetramethyluronium tetrafluoroborate, HOBt, and *N*,*N*-diisopropylethylamine (DIEA) (2.45:3:6). The Fmoc deprotection step was accomplished by treatment with 20% piperidine in DMF or by 2% 1,8-diazabicyclo[5.4.0]undec-7-ene (DBU) in DMF containing 2% piperidine for 2–3 min[24] to prevent the potential migration of Dde and DMab groups to other functional groups after the incorporation of Fmoc-DLys(Dde)-OH or/and Fmoc-Glu(DMab)-OH. Regarding analogs XVI, XVII, and XVIII after the removal of the DMab and/or Dde protecting groups by 2% hydrazine in DMF (3 × 2 min), on-resin acetylation of the N^{a}-amino group of Glu^{1} (peptide XVIII) and of N^{ε}-amino group of Lys^{8} (peptides XVI, XVII and XVIII) was performed by 0.5*M* Ac_2O in DMF for 1 h. The resin was washed manually with DMF, dichloromethane (DCM), and diethyl ether successively to remove the solvents excess. The peptidyl resin was treated with the splitting mixture trifluoroacetic acid (TFA)/DCM/anisole/1,2-ethanedithiol (EDT)/H_2O (92:3:2:1:2, v/v/v/v/v), for 3 h to remove the protecting groups and the peptide from the resin. The resin was filtered off, and the solution was concentrated. Peptides were isolated by precipitation with cold diethyl ether, centrifuged, dissolved in water with a few drops of acetic acid, and lyophilized. Purification of crude peptides was achieved by semipreparative HPLC (Mod.10 ÄKTA, Amersham Biosciences) on Supelcosil C18 (5 μm particle size, 8 mm × 250 mm, Sigma-Aldrich) Analytical HPLC (Waters, Malva) equipped with a Waters C18 column (symmetry, 3.5 μm, 4.6 mm × 75 mm) produced single peaks with at least 98% of the total peak integrals (integrated with Empower software). ESI-MS (Micromass-Platform LC instrument, Waters Micromass Technologies) was in agreement with the expected mass. The physicochemical properties of the new analogs are summarized in Table I.

Cyclic Peptides. The precyclic peptides (analogs XIV, XV, XX, XXI) were synthesized on a Sieber amide resin (0.45 mmol/g capacity) utilizing a standard Fmoc solid-phase synthesis protocol described above. Fmoc-protected peptidyl resins were treated with 2% DBU in DMF containing 2% piperidine for 2–3 min. Boc-protecting group was inserted on the free terminal amino group of the XIV and XX after treatment with $(Boc)_2O$ (3 equiv.)/DIEA (3 equiv.) in DMF (1 h, RT) while, on-resin N-terminal acetylation of the peptides XV and XXI was performed by using 0.5*M* Ac_2O in DMF for 1 h. After that step, Dde and DMab protecting groups were removed by using 2% hydrazine in DMF (3 × 2 min). Then, the amide bond between γ-carboxyl group of Glu^{1} and the ε-amino group of Lys in position 8 (analogs XIV, XV) or in position 5 (analogs XX, XXI) was carried out on the resin, using a mixture of PyBoP/HOBt/DIEA (1.5 equiv./1.5 equiv./2.0 equiv, 3 × 4 h, RT-60°C), monitoring the formation of the lactam bridge by Kaiser test. Cleavage from the resin and deprotection of the amino acid side chains of the cyclopeptides were performed as reported above. The resin was filtered off, and the solution was concentrated. The crude product was precipitated with cold diethyl ether, centrifuged, and lyophilized. Cyclopeptides were analyzed by analytical RP-HPLC and characterized using the procedure described above. The

physicochemical properties of the new analogs are summarized in Table I.

All peptides were purified by semipreparative HPLC on a RP C-18 support using a linear gradient from 20% to 35% of solvent A (0.1% TFA/H_2O) and solvent B (0.1% TFA/acetonitrile) for 15 min at a 2 mL/min flow rate and UV detection at 215 and 280 nm. Eluted peptides were lyophilized immediately. The purity of each peptide was verified by an analytical using a reversed-phase C18 column at a 1 mL/min flow rate with the same solvent system as in the preparative HPLC. The molecular weight of the peptides was confirmed by using ESI-MS. The HPLC chromatogram showed that the purity of the peptides was >98%, while ESI-MS showed the correct molecular ion for the peptide.

Cell Culture and Proliferation Assay

The human prostate cancer epithelial cell lines PC3 and LNCaP (ATCC, American Type Culture Collection) were grown in RPMI-1640 medium supplemented with 10% fetal bovine serum (FBS), 100 U/mL penicillin, and 100 μg/mL streptomycin. Cultures were maintained in 5% CO_2 and 100% humidity at 37°C. Cell culture reagents were from BiochromKG (Seromed, Germany).

Slow-growing LNCaP and fast-growing PC3 cells were seeded into 48-well culture plates at 1×10^4 cells/well. After a 24-h incubation period, adherent cells were treated with the peptides in 2.5% (v/v) FBS-RPMI-1640. At the end of the incubation period, cells were fixed with methanol and stained with 0.5% crystal violet in 20% methanol for 20 min.[25] After gentle rinsing with water, the retained dye was extracted with 30% acetic acid, and the absorbance was measured at 590 nm.

Comparison of mean values among groups was done using ANOVA and the unpaired Student *t*-test. Homogeneity of variance was tested by Levene's test. Each experiment included at least triplicate measurements for each condition tested. All results are expressed as the mean ± SD of at least three independent experiments. Values of P less than 0.05 were taken to be significant ($^*P < 0.05$, $^{**}P < 0.01$, $^{***}P < 0.001$).

NMR Spectroscopy

Samples of synthetic GnRH-I and 1GnRH-III in deuterated dimethyl sulfoxide (DMSO-d_6) were used for NMR studies. Data were acquired in a wide range of temperatures from 298 K up to 343 K on a Bruker Avance 400 MHz spectrometer. ^{1}H 1D NMR spectra were recorded using spectral width of 12–17 ppm with or without presaturation of the H_2O signal. ^{1}H-^{1}H 2D Total Correlation Spectroscopy (TOCSY)[26,27] were recorded using the MLEV-17 spin lock sequence using τ_m = 80–100 ms, and ^{1}H-^{13}C HSQC[28,29] spectra with 200.791 ppm spectral width in F1. ^{1}H-^{1}H TPPI Nuclear Overhauser Effect Spectroscopy (NOESY)[30,31] spectra were acquired using mixing time τ_m = 400 ms applying water suppression during the relaxation delay and mixing time. All 2D spectra were acquired with 10.014 ppm spectral width, consisting of 2K data points in the F2 dimension, 16–32 transients, and 512–1024 complex increments in the F1 dimension. Raw data were multiplied in both dimensions by a pure cosine-squared bell window function and Fourier-transformed to obtain 2048 × 2048 real data points. A polynomial baseline correction was applied in both directions. For data processing and spectral analysis, the standard Bruker software (XWinNMR 3.5) and XEASY program[32] (ETH, Zurich) were used.

NOE Constraints

Intensities of dipolar connectivities were mainly extracted by NOESY maps acquired at 298 K and 400 ms of mixing time. 409 and 299 NOESY cross-peaks were assigned in both dimensions for GnRH-I and 1GnRH-III peptides, respectively, in DMSO-d_6. The number of unique cross-peaks was 198 and 150 (20 and 15 NOEs per residue for GnRH-I and 1GnRH-III, respectively). Their intensities were converted into upper limit distances through CALIBA.[33] Sequential constraints, number and range of NOEs are illustrated in Supporting Information Figures S1 and S2.

Structure Calculations and Refinement

The NOE-derived structural information extracted from the analysis of NOESY spectra acquired in DMSO-d_6 solutions under identical experimental conditions for both peptides was introduced to DYANA[34,35] software for structure calculation. 113 and 87 NOE constraints for GnRH-I and 1GnRH-III, respectively, were found meaningful and used in DYANA calculations. A force constant of 133.76 kJ mol^{-1} Å^2 is applied for the distance constraints. The 20 models' ensembles of both GnRH peptides are illustrated in Figures 4 and 5 (Figures are generated with MOLMOL[36]). Structural calculations have been performed on IBM RISC6000 and xw4100/xw4200 HP Linux workstations.

RESULTS

Synthesis of Peptides

The application of Fmoc/tBu solid phase strategy combined with the appropriate side chain protecting groups resulted in the appropriate peptides with good yields of 40–81% (Table I). The preparation of side chain to side chain-cyclized peptides through lactam bridge formation requires orthogonal protecting groups for side chain amino and carboxylate functionalities. Our approach to acetylate or protect by the Boc protecting group the N-terminal amino group of the protected precyclic peptide was effective to prevent the potential formation of N^{α}-pyroglutamyl chain-terminated peptides, often favored during the deprotection step of Dmab group.[37]

Effect on Prostate Cancer Cell Proliferation

To study the anticancer activity of lGnRH-III and lGnRH-III analogs, we tested their effect on the anchorage-dependent proliferation of the well-established prostate carcinoma cell lines, LNCaP and PC3, that mimic different stages on the progression of prostate cancer. LNCaP cells are androgen-sensitive and express a large number of GnRHRs,[16,17] and PC3 cells are highly malignant, androgen-insensitive, and express lower number of GnRHrs.[6,38,39] lGnRH-III inhibited the proliferation of LNCaP cells in a concentration-dependent manner having a maximal effect (21.5% reduction) at the

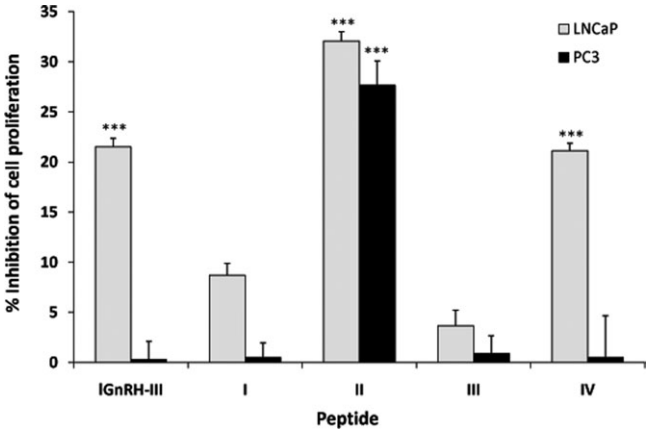

FIGURE 1 Effect of lGnRH-III and analogs I–IV on the proliferation of LNCaP and PC3 cells at a final concentration of 20 μM, after 144 h incubation for LNCaP cells and 96 h for PC3 cells. The cell number was estimated as described under Materials and Methods section. Results are presented as % inhibition relative to the control and are the mean ± SEM of three independent experiments. $^{***}P < 0.001$.

concentration of 20 μM. All analogs of lGnRH-III were tested at 20 μM concentration.

Analogs Modified in Position 6 (Group A)

[Asn^6]-lGnRH-III (analog I) and [Glu^6]-lGnRH-III (analog III) did not have significant inhibitory effect on LNCaP and PC3 cell proliferation whereas, the antiproliferative effect of analog [Gln^6]-lGnRH-III (IV) was similar to that of lGnRH-III. Substitution of Asp in position 6 by Asp(OMe) (peptide II) resulted in the most effective analog of that group (Figure 1); the inhibition effect on LNCaP cell proliferation, was higher compared to lGnRH-III (32.1 ± 0.9%, $P < 0.001$). Furthermore, while lGnRH-III was ineffective on PC3 cell proliferation, analog [Asp^6(OMe)]-lGnRH-III had significant (27.7 ± 2.1%, $P < 0.001$) antiproliferative effect.

Analogs with Modifications in Position 3 and/or 7 (Group B)

Analog [DTrp^3]-lGnRH-III (V) had increased antiproliferative activity on LNCaP cells and significant ($P < 0.001$) effect on PC3 cell proliferation compared to lGnRH-III, while substitution of Trp^7 by DTrp (analog VI) dramatically decreased the effect (no significant effect on both cell lines). Simultaneous incorporation of DTrp in positions 3 and 7 (analog VII) decreased the antiproliferative effect induced by analog V whereas, further modification of the C-terminal amide in analog [DTrp^3, DTrp^7]-lGnRH-III-NHEt (peptide VIII) increased it. Although analog [Tic^3, Tic^7]-lGnRH-III (IX) caused lower inhibition of LNCaP cell proliferation than that of lGnRH-III and significant ($P < 0.01$) effect on PC3 proliferation, incorporation of DTic in positions 3 and 7 (analog X) led to increased antiproliferative effect on both cancer cell lines (Figure 2). The antiproliferative effect of [DTrp^3, DTic^7]-lGnRH-III (analog XI) and [DTic^3, DTrp^7]-lGnRH-III (analog XII) was higher than that of lGnRH-III. In detail, analog XI inhibited the proliferation of LNCaP and PC3 cells by 36.5 ± 0.9% ($P < 0.001$) and 32.4 ± 4.0% ($P < 0.001$), respectively, and peptide XII, by 36.7 ± 0.7% ($P < 0.001$) and 31.6 ± 2.7% ($P < 0.001$), respectively.

Analogs with Amino Acid Changes in Positions 1, 5, 8 and Cyclic Compounds (Group C)

The antiproliferative effect of [NMeGlu^1]-lGnRH-III (analog XIII) on LNCaP cells was 30% lower than that of lGnRH-III whereas it had no effect on PC3 cell proliferation. Cyclic analogs [cyclo(Glu^1, Lys^8)]-lGnRH-III (XIV) and [cyclo(Ac-Glu^1, Lys^8)]-lGnRH-III (XV) had increased inhibitory effect on cell proliferation compared to lGnRH-III; their effect on LNCaP cells was 36.0 ± 2.0 ($P < 0.001$) and 35.8±1.0 ($P < 0.001$), respectively, while on PC3 cells the observed effect was 33.8 ± 2.0 ($P < 0.001$) and 30.6 ± 3.0 ($P < 0.001$), respectively (Figure 3). Acetylation of N^{ε} amino group of Lys^8 (analog XVI) led to significant increase in antiproliferative effect on both cell lines compared to lGnRH-III. Interestingly, further modifications on that analog in position 1 (analogs XVII and XVIII) decreased the effect on LNCaP cell proliferation compared to [ε-*N*-Ac-Lys^8]-lGnRH-III (Figure 3). On PC3 cell line, analog XVII had similar and XVIII had higher effect than analog with simple acetylation of N^{ε} amino group of Lys^8. Analog XIX {[Lys^5, His^8]-lGnRH-III} resulting

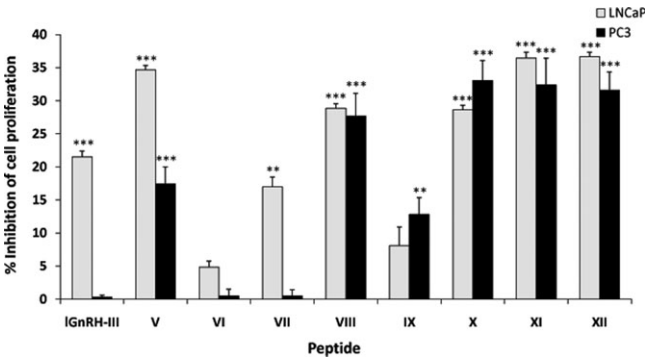

FIGURE 2 Effect of lGnRH-III and analogs V–XII on the proliferation of LNCaP and PC3 cells at a final concentration of 20 μM, after 144 h incubation for LNCaP cells and 96 h for PC3 cells. The cell number was estimated as described under Materials and Methods section. Results are presented as % inhibition relative to the control and are the mean ± SEM of three independent experiments. $^{**}P < 0.01$; $^{***}P < 0.001$.

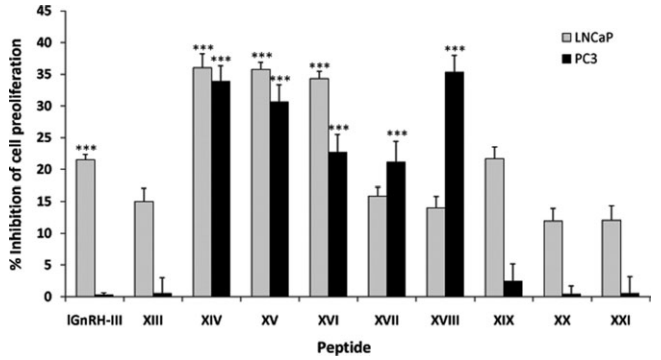

FIGURE 3 Effect of lGnRH-III and analogs XIII–XXI on the proliferation of LNCaP and PC3 cells at a final concentration of 20 μM, after 144 h incubation for LNCaP cells and 96 h for PC3 cells. The cell number was estimated as described under Materials and Methods section. Results are presented as % inhibition relative to the control and are the mean ± SEM of three independent experiments. $^{***}P < 0.001$.

after an exchange of positions between the two basic amino acids, His and Lys, had similar effect to lGnRH-III on LNCaP and PC3 proliferation. The antiproliferative effect on LNCaP cells of 1-5 cyclic analogs XX and XXI was lower than that of lGnRH-III and evidently decreased compared to counterparts 1-8 cyclic analogs (XIV and XV, Figure 3).

NMR Studies

Resonance Assignment. TOCSY maps of GnRH-I and 1GnRH-III peptides were first analyzed to assign the individual spin patterns of amino acids through scalar connectivities (Figure 4). Sequential, medium-, and long-range connectivities were identified from NOESY maps acquired with $\tau_m = 400$ ms. Proton chemical shift peptides are reported in Supporting Information Tables S1 and S2.

As far as the GnRH-I peptide is concerned, NH—NH connectivities of the type $(i,i+1)$ are detected for the region spanning the residues His^2-Leu^7 while NH—NH $(i,i+2)$ NOE cross-peaks are detected for the residue pairs His^2-Ser^4, Trp^3-Tyr^5, Tyr^5-Leu^7, and Arg^8-Gly^{10}. On the other hand, H_α—NH connectivities of the type $(i,i+1)$ are observed for the fragments $pGlu^1$-Tyr^5 and between the residues Leu^7-Arg^8, while H_β—NH type $(i,i+1)$ connectivities have been observed for the N-terminal tetra-peptide segment ($pGlu^1$-Ser^4) and for the Tyr^5-Gly^6 pair. Moreover, H_α—NH $(i,i+2)$ NOEs are identified among amino acids almost all over the peptide sequence. More than 30 medium-range NOEs were observed in the NOESY maps acquired with $\tau_m = 400$ ms. The most characteristics among them are H_β—NH type connectivities between amino acids Ser^4-Gly^6 and protons of the aromatic ring of His^2 with all backbone protons of Ser^4 as well as NOEs between Leu^7-Gly^{10} and Tyr^5-Arg^8. Long-range NOE signals involve the amide proton of N-terminal Serine at position 4 of the peptide sequence and the C-terminal Proline at the position 9 (four NOEs) as well as the amine protons of the CO-NH_2 terminal group (one NOE). These data provide a solid experimental evidence for the spatial proximity of the peptide's termini.

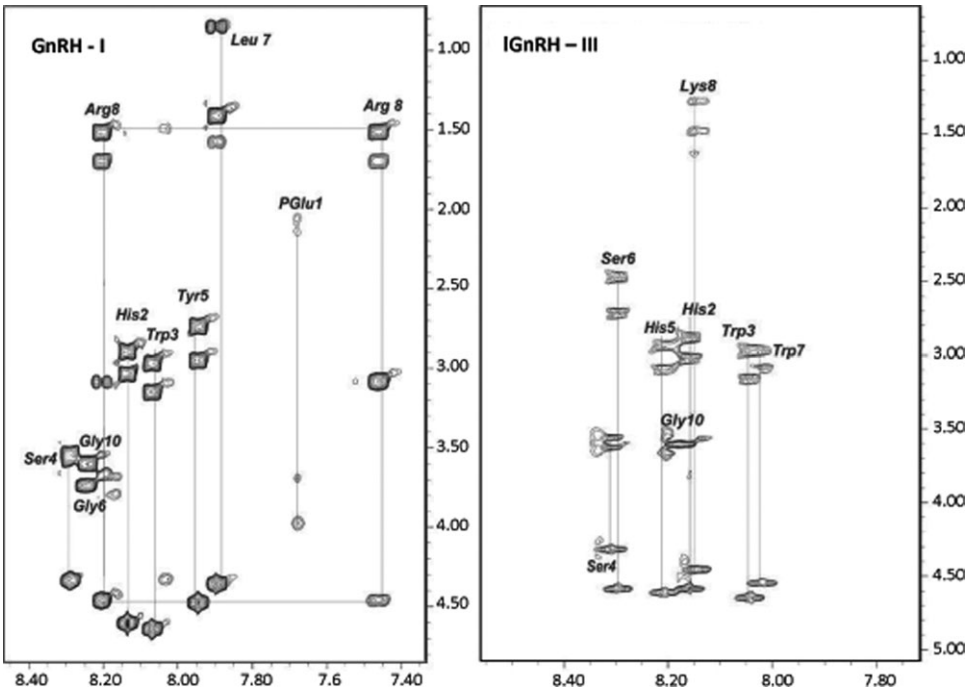

FIGURE 4 Characteristics ^1H-^1H TOCSY fingerprint regions of GnRH-I and 1GnRH-III peptides recorded at 400 MHz NMR and in DMSO-d_6 at 298 K.

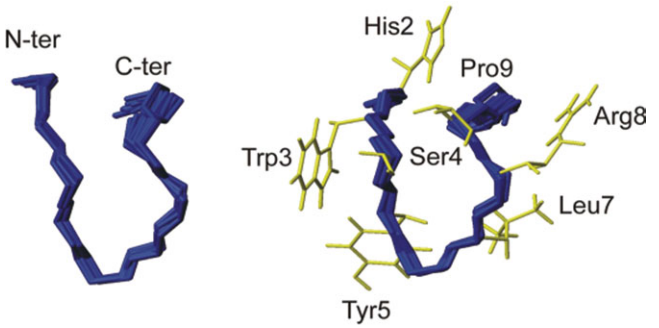

FIGURE 5 Backbone representation of the family of 20 energy minimized DYANA models calculated for the GnRH-I peptide illustrated in blue. Side chains are illustrated in yellow. Figures are generated with MOLMOL.

Although the 1GnRH-III exhibits a lower number of NOE cross-peaks compared to the GnRH-I, the number of identified NOEs is satisfactory, and 1GnRH-III can be defined by a single well-determined structure. The NOE pattern involving NH—NH connectivities, spanning the residues His^2-Lys^8, for this peptide is rather similar to these of the GnRH-I analog, while H_α—NH and H_β—NH ($i,i+1$) type connectivities have been identified all over the peptide sequence except for Pro^9. Both long- and medium-range NOEs involving backbone protons present in GnRH-I were totally absent in the 1GnRH-III analog. Only two H_β—H_β ($i,i+2$) type connectivities among Trp^3 and His^5 as well as one NOE cross-peak between the εNH of Lys^8 and the H_β of Asp^6 have been assigned. Moreover, the interaction among the aromatic rings of His^5 and Trp^7 is manifested by the existence of two medium-range NOEs between the H_ε proton of His^5 and the Hδ proton of Trp^7.

Structure Calculation and Conformational Analysis

The NOE-derived structural information extracted from the analysis of NOESY spectra acquired in DMSO under identical experimental conditions (τ_m = 400 ms) was introduced to DYANA for structure calculations. The average target function for the DYANA family of 20 calculated models was found $9.2 \times 10^{-2} \pm 1.7 \times 10^{-2}$ Å^2 for GnRH-I and $0.36 \pm 1.64 \times 10^{-3}$ Å^2 for 1GnRH-III, respectively. No consistent violations existed at the final DYANA run, and no constraint violation was found larger than 0.20 Å. The RMSD values for the GnRH-I 20 models' ensembles were calculated as 0.52 ± 0.24 Å (BB) and 0.96 ± 0.19 Å (HA). Similarly, the 1GnRH-III DYANA 20 models' ensembles exhibit pairwise RMSD values for all residues 0.70 ± 0.18 Å (BB) and 1.52 ± 0.60 Å (HA).

3D Solution Models

Despite the fact that a typical H_α—NH ($i,i+3$) connectivity has not been observed for the fragment Ser^4-Arg^8, the presence of the H_α—NH and NH—NH ($i,i+2$) connectivities—together with the absence of H_α—NH ($i,i+1$) type NOEs for Gly^6—suggest the existence of a β-turn structure in this region. In this conformation, the N-terminal region is close to the C-terminal and the spatial proximity of the two termini is manifested by long-range NOEs between: (i) the NH proton of Ser^4 and various Pro^9 protons, and (ii) the NH proton of the C-terminal amide. Since these long-range constraints might be fundamental for the β-turn formation and the convergence of the two peptides' termini, structure calculations were also performed without the above-mentioned long-range NOEs. The resulted ensemble of 20 DYANA models (PDB 1YY1) is also characterized by the formation of the β-turn and the highly flexible peptide termini. This conformation led us to conclude that the peptide preserves the hairpin-like conformation, and the NOE contacts that determine this conformation are all among the residues of the Ser^4-Arg^8 loop.

In the GnRH-I solution structure presented here, Gly^6 is found in the tip of the loop formed by residues Ser^4-Arg^8 (Figure 5). NOEs of ($i,i+2$) between H_α Ser^4 and HN Gly^6 as well as Gly^6 H_α—HN Arg^8 indicate that achiral Glycine residue in position 6 allows the turn formation and the U-shape fold of the peptide. Additionally, the side chains of Tyr^5 and Leu^7 seem to be in a short distance, while the observed NOEs between the Tyr^5 aryl protons and the Leu^7 methyl protons support the parallel orientation of their side chains. Moreover, the side chains of His^2 and Trp^3 present different orientation, while Trp^3 orients its indole ring to the same direction with the Tyr^5 aryl ring.

The substitution of the GnRH-I tetra-peptide segments Tyr^5-Gly^6-Leu^7-Arg^8, which is located in the middle of the GnRH-I sequence with the His^5-Asp^6-Trp^7-Lys^8 segment in 1GnRH-III, seems to impose great structural changes in the stereochemistry of the latter peptide. The spatial arrangement of both N- and C-terminal fragments is totally different with respect to the peptide representing the native hormone, since no long-range NOEs involving the terminal residues have been identified (Figure 6). Furthermore, there is no experimental evidence for a β-turn formation in the peptide segment 4-8, and consequently 1GnRH-III does not maintain the hairpin structure obtained in many GnRH analogs.[40,41] Despite the lower number of NOE cross-peaks identified in the NOESY spectra of 1GnRH-III, the peptide seems to adopt a rather defined backbone conformation. Our NMR data suggest that the molecule adopts extended backbone geometry with three irregular turns/bends around amino acids Trp^3, Ser^4, and Pro^9. The side chains of His^2 and Trp^3 still occupy different region in space, with the indole ring of Trp^3 found on the opposite site of the peptide backbone level in

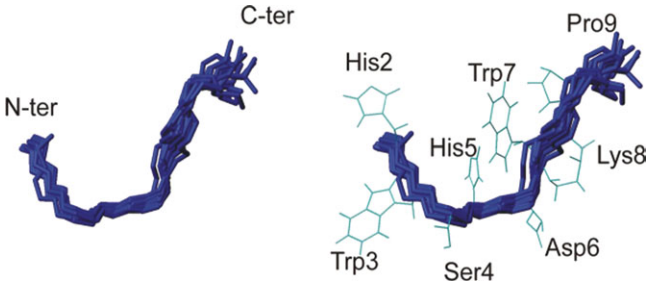

FIGURE 6 Backbone representation of the family of 20 energy minimized DYANA models calculated for the 1GnRH-III peptide illustrated in blue. Side chains are illustrated in cyan. Figures are generated with MOLMOL.

respect to the His^2 side chain and pointing towards the indole ring of Trp^7. Moreover, the aromatic ring of His^5 is found within NOE distance with Trp^7 indole ring supporting the parallel orientation of their side chains.

DISCUSSION

The ability of lGnRH-III to inhibit proliferation of cancer cells, combined with the weak GnRH-I agonistic activity, makes it an excellent starting compound for the development of peptide analogs with enhanced selectivity and anticancer activity. In this study, we report the synthesis of 21 new lGnRH-III analogs and their impact on the proliferation of two different prostate cancer cell lines. Moreover, to investigate the conformational resemblance or diversity in GnRH family, we studied the conformational properties of lGnRH-III and GnRH-I through NMR spectroscopy and their solution models are presented herein.

In our previous studies,[41] we have shown that GnRH-I does not exhibit significant antiproliferative activity on LNCaP and PC3 cells even at the concentration of 100 μM. Results of this study provide experimental evidence that the inhibitory effect of lGnRH-III, at the concentration of 20 μM, on LNCaP cell proliferation was 21.5 $\pm$ 0.9% while, on PC3 cell it was negligible. The absence of high affinity binding sites on PC3 cells[42] and the lower number of GnRHRs expressed on them[39] compared to LNCaP cells, may be related to the lack of responsiveness of PC3 cells following lGnRH-III treatment. However, many of the new analogs of lGnRH-III presented on this study had significant antiproliferative effect on both cancer cell lines. Our observations confirm the results of other studies that additional mechanisms may mediate the biological effects of GnRH analogs on cancer cells which have not yet been clarified.[42]

In lGnRH-III, the position 6 is occupied by Asp, whereas mammalian GnRH (GnRH-I) bears Gly at this position. Although Gly^6 is often replaced by D-amino acids to enhance the biological activity of GnRH-I analogs, previous studies report that removal of the Asp^6 in lGnRH-III resulted in complete loss of biological activity.[19,43] To further investigate the significance of this position, we substituted Asp^6 by Asn, Asp(OMe), Glu, and Gln. Incorporation of Asp(OMe) instead of Asp^6 significantly increased the antiproliferative activity of lGnRH-III on LNCaP cell line. Furthermore, Asp(OMe)-analog was the only analog of that group, with significant effect on PC3 proliferation. Insertion of Gln was well tolerated, while no antiproliferative activity on LNCaP cells was observed when Glu or Asn substitutes Asp^6. These findings suggest that neither the acidic function of the side chain of Asp^6 nor the putative salt bridge (Asp^6-Lys^8) are crucial for the antiproliferative activity of lGnRH-III, and we presume that different intramolecular interactions, that deserve further investigation, may occur and preserve the bioactive conformation.

According to Herédi-Szabó et al.,[19] indole rings of $Trp^{3,7}$ are crucial for the anticancer activity, probably due to interactions of these residues with the N-terminal which stabilizes the biological active conformation of lGnRH-III. In our study, the antiproliferative effect of the analog with DTrp in position 3 was significantly higher than lGnRH-III whereas $DTrp^7$ analog was ineffective. Introduction of DTrp instead of $Trp^{3,7}$ decreased the anticancer activity while, combined modification on the C-terminal resulted in a significant increase of the anticancer potency in both cancer cell lines. Tic is a conformationally restrained imino acid that has been incorporated to GnRH antagonists as local structure determinant.[44] In addition, we have previously shown that substitution of Trp^3 in GnRH-I by L- or D-Tic increased the antiproliferative effect of the analogs.[45] In this study, results show that substitution of $Trp^{3,7}$ by Tic decreases the antiproliferative effect of lGnRH-III on LNCaP cells and slightly improves the effect on PC3 cancer cells. In contrast, the inhibitory activity of the analogs [$DTic^{3,7}$]-lGnRH-III (X), [$DTrp^3$, $DTic^7$]-lGnRH-III (XI), and [$DTic^3$, $DTrp^7$]-lGnRH-III (XII) was significantly higher. Based on these findings, we presume that introduction of DTic, although lacks the indole ring, preserved the biologically active conformation of lGnRH-III. Furthermore, the importance of the stereochemistry of the residues in positions 3 and 7 is also indicated.

Conjugation of an acetyl-group via the side chain of Lys^8 significantly increases the antiproliferative activity of lGnRH-III suggesting that the putative salt bridge between Asp^6 and Lys^8 in lGnRH-III, proposed in an earlier structure activity study[16] and demonstrated by our findings, is not important for the anticancer activity. Similar elevation of the antiproliferative effect was observed by analogs with side chain

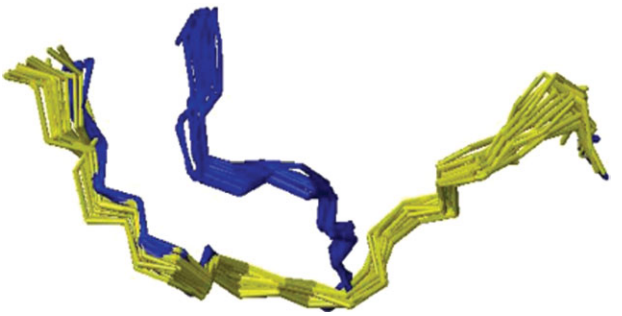

FIGURE 7 Superimposition of the backbone of the two hormones, lGnRH-III is illustrated in yellow while GnRH-I in blue. The calculated RMSD of both peptides for the segment 1-6 found to be 0.815Å.

cyclization of amino acids 1-8 (peptides XIV, XV) probably due to a more constrained conformation. On the other hand, although exchanging places between the weakly basic His^5 and the more basic Lys^8 did not alter the anticancer activity of the parent hormone, simultaneous 1-5 side chain cyclization in analogs XX and XXI resulted in lower antiproliferative effect.

In our attempt to elucidate conformational characteristics of lGnRH-III, the solution model was determined through NMR spectroscopy in DMSO, a solvent widely used for solubility reasons and is an acceptable medium of mimicking a prototypical hydrophobic environment. Furthermore, the 3D solution model of GnRH-I was also determined to shed light on the conformational differences between the two peptides. The obtained results show substantially different conformational features between the 1GnRH-III and the GnRH-I (Figure 7). According to our NMR study, the network of sequential NOE connectivities present in GnRH-I spectra suggest the existence of β-turn structure for the Ser^4-Arg^8 segment. Long-range NOE signals between the N- and C-termini provide solid experimental evidence for the spatial proximity of the two termini. On the other hand, 1GnRH-III does not exhibit the GnRH-I conformation (U-shape). In spite of earlier publications suggesting the existence of some helical properties,[23] such backbone conformation cannot be supported by our results. In contrast, the 3D models of 1GnRH-III can be characterized by the extended backbone conformation forming a kink around Asp^6 and two more turns/bends around Trp^3 and Pro^9. The present lGnRH-III models are in agreement with Mezo et al.,[17] where a relatively ordered extended like backbone conformation is proposed for the central region of the 1GnRH-III peptide.

The substitution of the small and flexible residue Gly in position 6 of the GnRH-I sequence with Asp^6 in 1GnRH-III does not favor the formation of the β-type conformation in the 4-8 segment of the peptide sequence. Moreover, the substitution of Leu^7 with the bulky Trp^7 differentiates remarkably the conformation of the peptide. This also becomes evident by the observed NOE interactions between His^5 and Trp^7, which do not favor the spatial proximity of the two termini. As a consequence, the hydrophobic core present in GnRH-I, is lost in 1GnRH-III.

Furthermore, the proposed ionic interaction between Asp^6-Lys^8 residues[16] is in agreement with our findings. Trp^7 changes its orientation pointing away from Lys^8 and consequently no NOE interaction is found between their side chains (as in the Leu^7-Arg^8 case in GnRH-I), and Asp^6 is found to be within NOE distance with Lys^8 giving rise to one interaction between εNH of Lys^8 and Hβ of Asp^6.

In conclusion, we synthesized 21 new lGnRH-III analogs and the structure–activity studies show that several of them had similar or higher activity than that of the parent hormone. Analogs II, V, VIII, X, XI, XII, XIV, XV, and XVI had higher antiproliferative activity than lGnRH-III on LNCaP cells and significant activity on PC3 cell. The modifications of those vary significantly but their inhibitory effect is almost the same, hampering thus the identification of one particular "lead compound." However, we have studied "key" positions of lGnRH-III, providing new information regarding the structure–activity relationship of lGnRH-III. Our observations are illustrating that lGnRH-III is a promising molecule for the development of peptide analogs with increased and potentially selective anticancer activity.

REFERENCES

1. Millar, R.P.; Pawson, A.J.; Morgan, K.; Rissman, E.F.; Lu, Z.L. Front Neuroendocrinol 2008, 29, 17–35.
2. Morgan, K.; Stewart, A.J.; Miller, N.; Mullen, P.; Muir, M.; Dodds, M.; Medda, F.; Harrison, D.; Langdon, S.; Millar, R.P. Cancer Res 2008, 68, 6331–6340.
3. Santen, R.J.; Manni, A.; Harvey, H. Breast Cancer Res Treat 1986, 7, 129–145.
4. Limonta, P.; Moretti, R.M.; Marelli, M.M.; Motta, M. Front Neuroendocrinol 2003, 24, 279–295.
5. Sower, S.A.; Chiang, Y.C.; Lovas, S.; Conlon, J.M. Endocrinology 1993, 132, 1125–1131.
6. Nozaki, M.; Ominato, K.; Gorbman, A.; Sower, S.A. Gen Comp Endocrinol 2000, 118, 57–67.
7. Tobet, S.A.; Nozaki, M.; Youson, J.H.; Sower, S.A. Cell Tissue Res 1995, 279, 261–270.
8. Yu, W.H.; Karanth, S.; Sower, S.A.; Parlow, A.F.; McCann, S.M. Proc Soc Exp Biol Med 2000, 224, 87–92.
9. Dees, W.L.; Hiney, K.K.; Sower, S.A.; Yu, W.H.; McCann, S.M. Peptides 1999, 20, 1503–1511.
10. McCann, S.M.; Karanth, S.; Mastronardi, C.A.; Dees, W.L.; Childs, G.; Miller, B.; Sower, S.; Yu, W.H. Arch Med Res 2001, 32, 476–485.

11. Yu, W.H.; Karanth, S.; Walczewska, A.; Sower, S.A.; McCann, S.M. Proc Natl Acad Sci USA 1997, 94, 9499–9503.
12. Sower, S.A. J Great Lakes Res 2003, 29 (suppl 1), 50–65.
13. Kovács, M.; Seprödi, J.; Koppán, M.; Horváth, J.E.; Vincze, B.; Teplán, I. J Neuroendocrinol 2002, 14, 1–14.
14. Amstalden, M.; Zieba, D.A.; Garcia, M.R.; Stanko, R.L.; Welsh, T.H., Jr.; Hansel, W.H. Reproduction 2004, 127, 35–43.
15. Lovas, S.; Pályi, I.; Vincze, B.; Horváth, J.; Kovács, M.; Mezö, I. J Pept Res 1998, 52, 384–389.
16. Mezö, I.; Lovas, S.; Pályi, I.; Vincze, B.; Kálnay, A.; Turi, G.; Vadász, Z.; Seprödi, J.; Idei, M.; Tóth, G.; Gulyás, E.; Otvös, F.; Mák, M.; Horváth, J.E.; Teplán, I.; Murphy, R.F. Med Chem 1997, 40, 3353–3358.
17. Mezo, G.; Czajlik, A.; Manea, M.; Jakab, A.; Farkas, V.; Majer, Z.; Vass, E.; Bodor, A.; Kapuvári, B.; Boldizsár, M.; Vincze, B.; Csuka, O.; Kovács, M.; Przybylski, M.; Perczel, A.; Hudecz, F. Peptides 2007, 28, 806–820.
18. Lovas, S.; Palyi, I.; Vincze, B.; Horvath, J.; Kovacs, M.; Mezo, I.; Toth, G.; Teplan, I.; Murphy, R.F. J Pep Res 1998, 52, 384–389.
19. Herédi-Szabó, K.; Lubke, J.; Tóth, G.; Murphy, R.F.; Lovas, S. Peptides 2005, 26, 419–422.
20. Iwai, H.; FEBS Lett 1999, 459, 166–172.
21. Gilon, C.; Mang, C.; Lohof, E.; Friedler, A.; Kessler, H. Synthesis of Peptides and Peptidomimetics, Goodman, M.; Toniolo, C.; Moroder, L.; Felix, A., Eds.; Georg Thieme Verlag: Stuttgart, 2003; pp 422–529.
22. Liu, C.F.; Rao, C.; Tam, J.P. Peptides: Frontiers of peptide science. Tam, J.P.; Kaumaya, P.T.P.; Eds.; Kluwer Academic Publishers: Dordrecht, The Netherlands, 1999; pp 235–237.
23. Watts, C.R.; Mezei, M.; Murphy, R.F; Lovas, S. J Biomol Struct Dyn 2001, 18, 733–748.
24. Augustyns, K.; Kraas, W.; Jung, G. J Pept Res 1998, 51, 127–133.
25. Nagakawa, O.; Fujiuchi, Y.; Fuse, H.; Saiki, I. Urology 2003, 62, 553–558.
26. Braunschweiler, L.; Ernst, R.R. J Magn Reson 1983, 53, 521–528.
27. Bax, A.; Davis, D.G. J Magn Reson 1985, 65, 355–360.
28. Bax, A.; Grzesiek, S. Acc Chem Res 1993, 26, 131–138.
29. Bothner-By, A.A.; Stephens, R.L.; Lee, J.C.; Warren, C.D.; Jeanloz, R.W. J Am Chem Soc 1984, 106, 811–813.
30. Marion, D.; Wuthrich, K. Biochem Biophys Res Commun 1983, 113, 967–974.
31. Jeener, J.; Meier, B.; Bachmann, P.; Ernst, R.R. J Chem Phys 1979, 71, 4546–4553.
32. Eccles, C.; Guntert, P.; Billeter, M.; Wuthrich, K.J. Biomol NMR 1991, 1, 111–130.
33. Guntert, P.; Braun, W.; Wuthrich, K. J Mol Biol 1991, 217, 517–530.
34. Guntert, P.; Mumenthaler, C.; Wuthrich, K. J Mol Biol 1997, 273, 283–298.
35. Wuthrich, K.; Billeter, M.; Braun, W. J Mol Biol 1983, 169, 949–961.
36. Koradi, R.; Billeter, M.; Wuthrich, K. J Mol Graph 1996, 14, 51–55, 29–32.
37. Johnson, T.; Liley, M.; Cheeseright, J.T.; Begum, F.J. Chem Soc Perkin Trans 1 2000, 16, 2811–2820.
38. Alimirah, F.; Chena, J.; Basrawalab, Z.; Xina, H.; Choubey, D. FEBS Lett 2006, 580, 2294–2300.
39. Kraus, S.; Levy, G.; Hanoch, T.; Naor, Z.; Seger, R.M. Cancer Res 2004, 64, 5736–5744.
40. Tare, R.S.; Oreffo, R.O.; Sato, K.; Rauvala, H.; Clarke, N.M.; Roach, H.I. Biochem Biophys Res Commun 2002, 298, 324–332.
41. Pappa, E.V.; Zompra, A.A.; Spyranti, Z.; Diamantopoulou, Z.; Pairas, G.; Lamari, F.N.; Katsoris, P.; Spyroulias, G.A.; Cordopatis, P. Biopolymers 2011, 96, 260–272.
42. Ravenna, L.; Salvatori, L.; Morrone, S.; Lubrano, C.; Cardillo, MR.; Sciarra, F.; Frati, L.; Di Silverio, F.; Petrangeli, E. J Androl 2000, 21, 549–557.
43. Kovács, M.; Vincze, B.; Horváth, J.E.; Seprödi, J. Peptides 2007, 28, 821–829.
44. Koerber, S.C.; Ibea, M.; Hagler, A.T.; Rivier, C.L; Rivier, J.E. Biochem Biophys Res Commun 1992, 187, 1035–1041.
45. Zompra, A.A.; Magafa, V.; Lamari, F.N.; Nock, B.; Maina, T.; Spyroulias, G.A.; Karamanos, N.K.; Cordopatis, P. J Pept Res 2005, 1, 57–64.